A Novel Approximate Antenna Pattern for Directional Antenna Arrays

Na Deng and Martin Haenggi, *Fellow, IEEE*

***Abstract*—The antenna pattern model plays a key role in evaluating the performance benefits of directional antenna arrays. In this letter, we propose a novel antenna pattern, named *multi-cosine antenna pattern*, to approximate the actual antenna pattern, and apply it to millimeter wave (mm-wave) networks. To get deep insights on the role of directional antenna arrays in mm-wave networks, we derive exact expressions for the success probability of the typical receiver as well as a tight upper bound. The results show that the proposed antenna pattern provides a better tradeoff between the accuracy and the tractability in terms of both antenna pattern and analysis than previous models.**

***Index Terms*—Directional antenna arrays, antenna pattern approximation, mm-wave, success probability, stochastic geometry.**

I. Introduction

Millimeter-wave (mm-wave) communications is considered a promising enabling technology for future networks, where directional transmissions with large-scale antenna arrays is one of its key distinguishing features to cope with the huge propagation losses. In mm-wave networks, since the desired signal and the interference power are highly directional and closely related to the angles of departure/arrival (AoDs/AoAs), directional antenna arrays will dramatically affect the desired signal and the interference power due to the various power gains for different AoDs/AoAs. Therefore, it is necessary and critical to adopt an accurate yet tractable antenna pattern model when analyzing mm-wave networks.

To maintain analytical tractability, previous works on mm-wave network analysis usually considered the uniform linear array (ULA)[1] and adopted a *flat-top* pattern, also named *sectorized* antenna model, to approximate the actual antenna pattern, see, e.g., [1] and references therein. While this model leads to relatively simple analytical results, its binary quantization of the continuously varying antenna array gains causes significant deviations from the actual performance [2]. To generalize the flat-top pattern from the binary version to an M-ary quantization, a multi-lobe approximation was proposed in [3] as a fine-grained model, where the array gain and the width of each lobe are obtained through minimizing the error function between the multi-lobe pattern and the actual one. However, the main lobe gain of the multi-lobe pattern is lower than the maximum array gain of the actual pattern, thus underestimating the desired signal strength. Moreover, the multi-lobe model cannot reflect the roll-off characteristic of the actual antenna pattern, especially for large antenna arrays. As a result, such inaccuracy of the multi-lobe approximation would still lead to deviations on the network performance.

Very recently, two other approximate antenna patterns are proposed in [2], named sinc and cosine antenna patterns. While the sinc pattern provides a more accurate approximation than the flat-top pattern, the analysis and its numerical evaluation are more complicated with little insights. The cosine pattern, with better analytical tractability than the sinc pattern, provides a good approximation for the main lobe gains while neglecting the side lobe ones. As the network density increases, the aggregated interference from the side lobes becomes stronger and stronger, thus leading to severe underestimation of the interference and deviation on the network performance. Two more antenna patterns (patch and horn) [4, Chap. 13-14] are adopted in [5]. They permit a tractable analysis but make it difficult to characterize the effect of the array size on the performance since the array gain is just a function of the signal direction.

In this letter, we propose a new approximate antenna pattern for the ULA, named *multi-cosine pattern*, which strikes a good balance between accuracy and tractability for mm-wave networks. With this antenna pattern at hand, we give exact expressions for the success probability as well as a tight upper bound using tools from stochastic geometry.

II. System Model

A. Multi-Cosine Antenna Pattern

Let $\varphi = \frac{d_\mathrm{t}}{\varrho}\cos\phi$ be the cosine direction corresponding to the AoD ϕ of the transmit signal, termed the *spatial AoD*, with d_t and ϱ representing the antenna spacing and wavelength, respectively. The actual antenna pattern of the ULA [2] is

$$G_{\mathrm{act}}(\varphi) = \frac{\sin^2(\pi N\varphi)}{N\sin^2(\pi\varphi)}. \tag{1}$$

d_t is usually set to be half-wavelength to enhance the directionality of the beam and avoid grating lobes; φ is assumed to be uniformly distributed in $[-0.5, 0.5]$, and thus the spatial AoD from an interferer to the typical receiver is also uniformly distributed in $[-0.5, 0.5]$, as proven in [2]. Due to the even symmetry of φ, it suffices to focus on the non-negative interval $\varphi \geq 0$. The side lobe width is $1/N$, and the maxima of side

Na Deng is with the School of Information and Communication Engineering, Dalian University of Technology (DLUT), Dalian, 116024, China (e-mail: dengna@dlut.edu.cn). Martin Haenggi is with the Dept. of Electrical Engineering, University of Notre Dame, Notre Dame 46556, USA (e-mail: mhaenggi@nd.edu).

This work was supported by the National Natural Science Foundation of China under Grant 61701071, the China Postdoctoral Science Foundation (2017M621129), the Fundamental Research Funds for the Central Universities (DUT16RC(3)119), and the US NSF grant CCF 1525904.

[1]The ULA can be easily extended to other general cases, e.g., the uniform rectangular array.

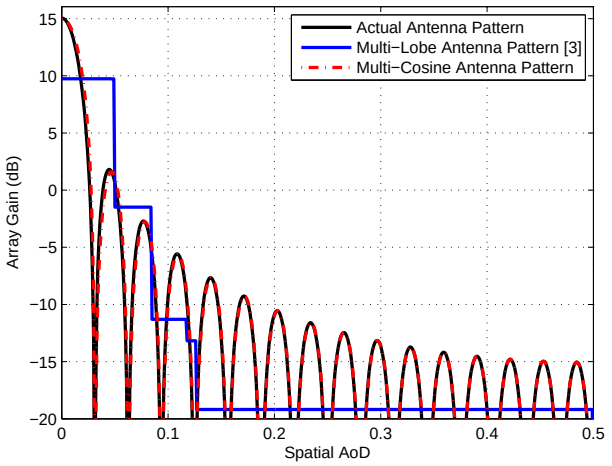

Fig. 1. Visualization of three different antenna patterns for $N = 32$.

lobes in the positive interval occur approximately when the numerator of (1) attains its maximum value, i.e., $\varphi_k = \frac{2k+1}{2N}$, $k \in [K], K = \left\lfloor \frac{N}{2} \right\rfloor - 1$.

Since the cosine pattern matches the main lobe well, it is intuitive to model the side lobes with multiple scaled and shifted cosine patterns. Thus, we propose a multi-cosine antenna pattern to approximate the actual antenna pattern.

Definition 1. (Multi-cosine antenna pattern) *The multi-cosine antenna pattern is given by*

$$G(\varphi) = \begin{cases} G_0 \cos^2\left(\frac{\pi N}{2}\varphi\right) & \text{if } |\varphi| \le \frac{1}{N} \\ G_k \cos^2\left(\pi N(|\varphi| - \varphi_k)\right) & \text{if } \frac{k}{N} < |\varphi| \le \frac{k+1}{N} \\ 0 & \text{otherwise,} \end{cases} \quad (2)$$

where $G_k = G_{\text{act}}(\varphi_k)$ *for* $k > 0$ *and* $G_0 = N$.

Fig. 1 compares the multi-cosine, the multi-lobe as well as the actual antenna patterns. It turns out that the multi-cosine pattern matches the actual one extremely well and is more accurate than the multi-lobe one since it captures the roll-off characteristics of both the main and the side lobes. Moreover, as N increases, the array gains will vary dramatically with different AoDs. In the multi-lobe pattern, however, it is difficult to accurately track such variations because there is no explicit relationship between the array gain and the array size, and increasing the number of lobes will significantly increase the difficulty in solving the nonlinear problem to obtain its parameters.

B. Network Model

To illustrate the desirable properties of the antenna model, we consider a mm-wave communication network, where the transmitters are distributed according to a homogeneous Poisson point process (PPP) $\hat{\Phi}$ with density λ and each one has a dedicated receiver at distance r_0 in a random orientation[2]. We consider a receiver at the origin that attempts to receive from an additional transmitter located at $(r_0, 0)$. Due to Slivnyak's theorem [6, Thm. 8.10], this receiver becomes the typical receiver under expectation over the PPP. We assume that each receiver has a single antenna and its corresponding transmitter is equipped with a ULA composed of N elements. All transmitters operate at a constant power μ and apply analog beamforming with the assumption of perfect beam alignment. The ALOHA channel access scheme is adopted, i.e., in each time slot, transmitters in $\hat{\Phi}$ independently transmit with probability q.

[2]This is a *Poisson bipolar model* [6, Def. 5.8], which is usually used to model device-to-device and ad hoc networks.

C. Blockage and Propagation Model

The generalized LOS ball model [7] is used to capture the blockage effect in mm-wave communication. Specifically, the LOS probability of the channel between two nodes with separation d is

$$P_{\text{LOS}}(d) = p_{\text{L}} \mathbf{1}_{d<R}, \quad (3)$$

where $\mathbf{1}$ is the indicator function, R is the maximum length of a LOS channel, and the LOS fraction constant $p_{\text{L}} \in [0,\ 1]$ is the LOS probability if the distance d is less than R. The blockage effect induces different path loss exponents, denoted as α_{L} and α_{N}, for LOS and NLOS channels, respectively. We denote by $\ell(x)$ the random path loss function associated with the interfering transmitter location $x \in \hat{\Phi}$, given by

$$\ell(x) = \begin{cases} (\max\{d_0, |x|\})^{-\alpha_{\text{L}}} & \text{w.p. } P_{\text{LOS}}(|x|) \\ (\max\{d_0, |x|\})^{-\alpha_{\text{N}}} & \text{w.p. } 1 - P_{\text{LOS}}(|x|), \end{cases} \quad (4)$$

where all $\ell(x)_{x\in\hat{\Phi}}$ are independent.

We assume that the desired link between the transmitter-receiver pair is in the LOS condition with deterministic path loss $r_0^{-\alpha_{\text{L}}}$. In fact, if the receiver was associated with a NLOS transmitter, the link would quite likely be in outage due to the severe propagation loss and high noise power at mm-wave bands as well as the fact that the interferers can be arbitrarily close to the receiver. In addition to the distance-dependent path loss, we assume independent Nakagami fading, which is suitable in the LOS-dependent mm-wave scenarios. Different Nakagami fading parameters M_{L} and M_{N} are assumed for LOS and NLOS paths, where both are positive integers. The power fading coefficient between node $x \in \hat{\Phi}$ and the origin is denoted by h_x, which follows a gamma distribution $\text{Gamma}(M, \frac{1}{M})$ with $M \in \{M_{\text{L}},\ M_{\text{N}}\}$, and all h_x are mutually independent and also independent of $\hat{\Phi}$.

D. SINR Analysis

For the typical receiver, the interferers outside the LOS ball are NLOS and thus can be ignored due to the severe path loss over the large distance (at least R). As a result, we merely focus on the analysis of a finite network region, and the relevant transmitters, denoted as Φ, correspond to the PPP in a disk of radius R centered at the origin. Due to the incorporation of the blockages, the LOS transmitters with LOS propagation to the typical receiver form a PPP Φ_{L} with density $p_{\text{L}}\lambda$, while Φ_{N} with density $p_{\text{N}}\lambda$ is the transmitter set with NLOS propagation, where $p_{\text{L}}+p_{\text{N}} = 1$ such that $\Phi = \Phi_{\text{L}} \cup \Phi_{\text{N}}$.

Without loss of generality, the noise power is set to one, and the SINR at the typical receiver is

$$\text{SINR} \triangleq \frac{\mu N h_{x_0} r_0^{-\alpha_\text{L}}}{1+I}. \tag{5}$$

where $I = \sum_{x\in\Phi} \mu G(\varphi_x) h_x \ell(x) B(x)$ is the interference, $G(\varphi_x)$ follows from (2), and $B(x)$ is a Bernoulli variable with parameter q to indicate whether x transmits.

III. Analysis of Success Probability

The success probability $P(\theta) = \mathbb{P}(\text{SINR} \geq \theta)$ is the complementary cumulative distribution function of the SINR.

A. Exact Expression

Our first result is to compare the multi-cosine and actual patterns in terms of the total radiated power.

Lemma 1. *For all values of the network parameters, the success probability with the multi-cosine pattern (2) is a lower bound of the success probability with the actual pattern (1).*

Proof: For $n \in \mathbb{N}$, partition the interference at the receiver into the contributions I_i, $i \in [n]$, each coming from a sector of angle $2\pi/n$. Since the interferers form a PPP and their antennas are uniformly randomly oriented, the I_i are i.i.d. Hence the total interference is a weighted sum of i.i.d random variables, where each weighting factor corresponds to the antenna gain in that direction. Letting $n \to \infty$, the sum of the weighting factors becomes the integral over the antenna gain. From (1) and (2), we have

$$\int_{-0.5}^{0.5} G(\varphi)\mathrm{d}\varphi = 1 + \sum_{k=1}^{K} \frac{G_k}{N} > \int_{-0.5}^{0.5} G_\text{act}(\varphi)\mathrm{d}\varphi = 1. \tag{6}$$

Thus the interference of the multi-cosine pattern stochastically dominates that of the actual antenna pattern, which leads to a reduction in the success probability. ∎

Theorem 1. *Letting $\epsilon = \frac{M_\text{L} r_0^{\alpha_\text{L}}}{\mu N}$, the success probability of the typical active receiver, denoted by $P(\theta)$, is given by*

$$P(\theta) = \sum_{m=0}^{M_\text{L}-1} \frac{(-u)^m}{m!} \mathcal{L}^{(m)}(u)|_{u=\theta\epsilon}, \tag{7}$$

where $\mathcal{L}(u) = \exp(\eta(u))$, the superscript '$(m)$' stands for the m-th derivative of $\mathcal{L}(u)$, and

$$\eta(u) = -u - \sum_{s\in\{\text{L},\,\text{N}\}} p_s \lambda q \frac{2}{N}\left((K+1)\pi R^2 - \sum_{z=0}^{\infty} A_s(z) u^z\right), \tag{8}$$

where

$$A_s(z) = \sqrt{\pi}\binom{M_s+z-1}{z}\left(-\frac{\mu}{M_s}\right)^z \frac{\Gamma(z+1/2)}{z!} \times \frac{z\alpha_s d_0^{2-z\alpha_s} - 2R^{2-z\alpha_s}}{z\alpha_s - 2} \sum_{k=0}^{K} G_k^z. \tag{9}$$

$\mathcal{L}^{(m)}(u)$ is given recursively by

$$\mathcal{L}^{(m)}(u) = \sum_{n=0}^{m-1} \binom{m-1}{n} \eta^{(m-n)}(u) \mathcal{L}^{(n)}(u), \tag{10}$$

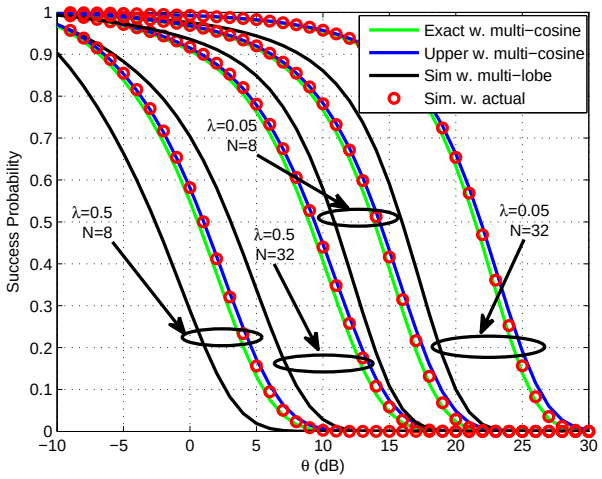

Fig. 2. The link success probabilities for different antenna patterns with $M_\text{L} = 4$, $M_\text{N} = 2$, $\alpha_\text{L} = 2.5$, $\alpha_\text{N} = 4$, $q = 0.5$, $d_0 = 1$, $r_0 = 2$, $\mu = 100$, $p_\text{L} = 0.2$ and $R = 200$.

where the n-th derivative of $\eta(u)$ follows

$$\eta^{(n)}(u) = \mathbf{1}_{n=1} + \sum_{s\in\{\text{L},\,\text{N}\}} \frac{2p_s\lambda q}{N} \sum_{z=n}^{\infty} \frac{\Gamma(z+1)A_s(z)u^{z-n}}{\Gamma(z-n+1)}. \tag{11}$$

Proof: See Appendix A.

B. Upper Bound on Success Probability

Although the Laplace transform of the aggregate interference can be easily evaluated by numerical integration, the corresponding n-th derivative needs tedious and extensive computations. Thus, we next derive a bound that is much easier to evaluate.

Theorem 2. *Let $\beta = [\Gamma(1+M_\text{L})]^{-1/M_\text{L}}$ and*

$$\hat{P}(\theta) = \sum_{m=1}^{M_\text{L}} \binom{M_\text{L}}{m} (-1)^{m+1} \mathcal{L}(u)\big|_{u=m\theta\beta\epsilon}. \tag{12}$$

For a Poisson bipolar mm-wave network, the success probability $P(\theta)$ is upper bounded by $\hat{P}(\theta)$.

Proof: It is known from [8] that

$$\widetilde{\Gamma}(M,x) \leq 1 - [1-\exp(-\beta x)]^M, \tag{13}$$

where $\beta = [\Gamma(1+M)]^{-1/M}$, $\widetilde{\Gamma}(M,x) = \Gamma(M,x)/\Gamma(M)$, and an upper bound on $P(\theta)$ is then given as

$$\begin{aligned}\hat{P}(\theta) &= 1 - \mathbb{E}\left[\left(1-\exp\left(-\theta\beta\epsilon(1+I)\right)\right)^{M_\text{L}}\right] \\ &= \sum_{m=1}^{M_\text{L}} \binom{M_\text{L}}{m} (-1)^{m+1} \mathbb{E}\left[\exp\left(-m\theta\beta\epsilon(1+I)\right)\right] \\ &= \sum_{m=1}^{M_\text{L}} \binom{M_\text{L}}{m} (-1)^{m+1} \mathcal{L}(u)\big|_{u=m\theta\beta\epsilon}. \end{aligned} \tag{14}$$

where $\beta = [\Gamma(1+M_\text{L})]^{-1/M_\text{L}}$. By substituting (8) into (14), we obtain the upper bound for the link success probability. ∎

Fig. 2 compares three antenna patterns in terms of the success probability. It is observed that the proposed multi-cosine

antenna pattern is much more accurate than the multi-lobe one and, in agreement with Lemma 1, leads to a lower bound. Both the exact results and the upper bounds approximate the success probability with the actual antenna pattern extremely well while the multi-lobe antenna pattern underestimates the success probability by 3-5 dB (horizontal gap) and causes increasingly large deviations with the increase of N. We also observe that the exact result becomes more accurate in the high-SINR regime while the upper bound yields a better approximation in the low-SINR regime.

IV. Conclusions

We proposed an accurate yet tractable approximation to the actual antenna pattern in mm-wave networks, named multi-cosine pattern, based on the cosine function with multiple shifted and scaled operations. Based on this antenna model, we derived exact expressions for the success probability as well as its upper bound for mm-wave ad hoc networks. The results demonstrate that the proposed multi-cosine antenna pattern provides extremely close approximations in terms of both the antenna pattern and the success probability.

Appendix A
Proof of Theorem 1

Proof: $P(\theta)$ is given by

$$\begin{aligned} P(\theta) &= \mathbb{E}\left[\widetilde{\Gamma}\left(M_{\mathrm{L}}, \theta\epsilon(1+I)\right)\right] \\ &= \sum_{m=0}^{M_{\mathrm{L}}-1} \mathbb{E}\left[e^{-\theta\epsilon(1+I)}\frac{(\theta\epsilon(1+I))^m}{m!}\right] \\ &= \sum_{m=0}^{M_{\mathrm{L}}-1} \frac{(-u)^m}{m!}\mathcal{L}^{(m)}(u)|_{u=\theta\epsilon}, \end{aligned} \tag{15}$$

where $\widetilde{\Gamma}(x,y) = \Gamma(x,y)/\Gamma(x)$ is the normalized incomplete gamma function, $\mathcal{L}(u) = \mathbb{E}[e^{-u(I+1)}]$ is the Laplace transform of the interference and noise, and the superscript (m) stands for the m-th derivative of $\mathcal{L}(u)$. Since the interference is from both LOS and NLOS interferers, we have

$$\mathcal{L}(u) = e^{-u}\prod_{s\in\{\mathrm{L},\,\mathrm{N}\}}\mathbb{E}_{I_s}e^{-uI_s} = e^{-u}\prod_{s\in\{\mathrm{L},\,\mathrm{N}\}}\mathcal{L}_{I_s}(u), \tag{16}$$

where $\mathcal{L}_{I_s}(u)$ follows as

$$\begin{aligned} &\mathcal{L}_{I_s}(u) \\ &= \mathbb{E}\left[\prod_{x\in\Phi_s}\left(\frac{q}{\left(1+u\mu G(\varphi_x)\ell_s(x)/M_s\right)^{M_s}}+1-q\right)\right] \\ &= \mathbb{E}_{\Phi_s}\Bigg[\prod_{x\in\Phi_s}\Bigg(\sum_{k=1}^{K}\int_{\frac{k}{N}}^{\frac{k+1}{N}}\frac{2q\mathrm{d}\varphi}{\left(1+\frac{u\mu G_k\cos^2(\pi N(\varphi-\theta_k))\ell_s(x)}{M_s}\right)^{M_s}} \\ &\quad +\int_{-\frac{1}{N}}^{\frac{1}{N}}\frac{q\mathrm{d}\varphi}{\left(1+\frac{u\mu N\cos^2(\pi N\varphi/2)\ell_s(x)}{M_s}\right)^{M_s}}+1-\frac{2q(K+1)}{N}\Bigg)\Bigg] \\ &= \exp\Bigg(-\frac{2p_s\lambda q}{N}\sum_{k=0}^{K}\Bigg(\pi R^2-\underbrace{\int_0^R\int_0^{\frac{\pi}{2}}\frac{4r\mathrm{d}y\mathrm{d}r}{\left(1+\frac{u\mu G_k\cos^2(y)\ell_s(r)}{M_s}\right)^{M_s}}}_{\mathcal{X}}\Bigg)\Bigg). \end{aligned} \tag{17}$$

Using the general binomial theorem, we have

$$\begin{aligned} \mathcal{X} &= 4\sum_{z=0}^{\infty}\binom{M_s+z-1}{z}\left(-\frac{u\mu G_k}{M_s}\right)^z\int_0^{\frac{\pi}{2}}\cos^{2z}(y)\mathrm{d}y\int_0^R\ell_s^z(r)r\mathrm{d}r \\ &= \sqrt{\pi}\sum_{z=0}^{\infty}u^z\binom{M_s+n-1}{z}\left(-\frac{\mu G_k}{M_s}\right)^z\frac{\Gamma(z+1/2)}{z!} \\ &\quad\times\frac{z\alpha_s d_0^{2-z\alpha_s}-2R^{2-z\alpha_s}}{z\alpha_s-2}. \end{aligned} \tag{18}$$

Letting

$$\begin{aligned} A_s(z) &= \sqrt{\pi}\binom{M_s+z-1}{z}\left(-\frac{\mu}{M_s}\right)^z\frac{\Gamma(z+1/2)}{z!} \\ &\quad\times\frac{z\alpha_s d_0^{2-z\alpha_s}-2R^{2-z\alpha_s}}{z\alpha_s-2}\sum_{k=0}^{K}G_k^z, \end{aligned} \tag{19}$$

$$\eta(u) = -u-\sum_{s\in\{\mathrm{L},\,\mathrm{N}\}}p_s\lambda q\frac{2}{N}\left((K+1)\pi R^2-\sum_{z=0}^{\infty}A_s(z)u^z\right), \tag{20}$$

we have $\mathcal{L}(u) = \exp(\eta(u))$. Since $\mathcal{L}^{(1)}(u) = \eta^{(1)}(u)\mathcal{L}(u)$, $\mathcal{L}^{(m)}(u)$ can be calculated recursively according to the formula of Leibniz, given by

$$\mathcal{L}^{(m)}(u) = \frac{\mathrm{d}^{m-1}\mathcal{L}^{(1)}(u)}{\mathrm{d}u} = \sum_{n=0}^{m-1}\binom{m-1}{n}\eta^{(m-n)}(u)\mathcal{L}^{(n)}(u),$$

where the n-th derivative of $\eta(u)$ follows as

$$\eta^{(n)}(u) = \mathbf{1}_{(n=1)}+\sum_{s\in\{\mathrm{L},\,\mathrm{N}\}}\frac{2p_s\lambda q}{N}\sum_{z=n}^{\infty}\frac{\Gamma(z+1)A_s(z)u^{z-n}}{\Gamma(z-n+1)}. \tag{21}$$

■

References

[1] J. G. Andrews, T. Bai, M. N. Kulkarni, A. Alkhateeb, A. K. Gupta, and R. W. Heath, "Modeling and analyzing millimeter wave cellular systems," *IEEE Transactions on Communications*, vol. 65, no. 1, pp. 403–430, Jan. 2017.

[2] X. Yu, J. Zhang, M. Haenggi, and K. B. Letaief, "Coverage analysis for millimeter wave networks: The impact of directional antenna arrays," *IEEE Journal on Selected Areas in Communications*, vol. 35, no. 7, pp. 1498–1512, Jul. 2017.

[3] M. D. Renzo, W. Lu, and P. Guan, "The intensity matching approach: A tractable stochastic geometry approximation to system-level analysis of cellular networks," *IEEE Transactions on Wireless Communications*, vol. 15, no. 9, pp. 5963–5983, Sept. 2016.

[4] C. A. Balanis, *Antenna Theory: Analysis and Design*. Hoboken, NJ, USA: John Wiley & Sons, 2005.

[5] O. Georgiou, "Simultaneous wireless information and power transfer in cellular networks with directional antennas," *IEEE Communications Letters*, vol. 21, no. 4, pp. 885–888, Apr. 2017.

[6] M. Haenggi, *Stochastic geometry for wireless networks*. Cambridge University Press, 2012.

[7] S. Singh, M. N. Kulkarni, A. Ghosh, and J. G. Andrews, "Tractable model for rate in self-backhauled millimeter wave cellular networks," *IEEE Journal on Selected Areas in Communications*, vol. 33, no. 10, pp. 2196–2211, Oct. 2015.

[8] H. Alzer, "On some inequalities for the incomplete gamma function," *Mathematics of Computation*, vol. 66, no. 66, pp. 771–778, 1997.